

See discussions, stats, and author profiles for this publication at: <https://www.researchgate.net/publication/20399702>

Molecular topography and secondary structure comparisons of botulinum neurotoxin types A, B and E

ARTICLE *in* MOLECULAR AND CELLULAR BIOCHEMISTRY · APRIL 1989

Impact Factor: 2.39 · DOI: 10.1007/BF00231693 · Source: PubMed

CITATIONS

19

READS

6

2 AUTHORS, INCLUDING:



Bal Ram Singh

Institute of Advanced Sciences

151 PUBLICATIONS 2,435 CITATIONS

SEE PROFILE

B.R. Singh
7/31/89

#13

Original Article

Molecular topography and secondary structure comparisons of botulinum neurotoxin types A, B and E

Bal Ram Singh and B. R. DasGupta

Food Research Institute, 1925 Willow Drive, University of Wisconsin, Madison, WI 53706, USA

Received 16 May 1988; accepted 5 October 1988

Key words: botulinum neurotoxin, derivative spectra, tyrosine exposure, secondary structure, circular dichroism

Abstract

Botulinum neurotoxin (NT) serotypes A, B and E differ in microstructure and biological activities. The three NTs were examined for secondary structure parameters (α -helix, β -sheet, β -turn and random coil content) on the basis of circular dichroism; degree of exposed Tyr residues (second derivative spectroscopy) and state of the Trp residues (fluorescence and fluorescence quantum yield). The proteins are high in β -pleated sheet content (41–44%) and low in α -helical content (21–28%). About 30–36% of the amino acids are in random coils. The β -sheet contents in the NTs are similar irrespective of their structural forms (i.e. single or dichain forms) or level of toxicity. About 84%, 58% and 61% of Tyr residues of types A, B, and E NT, respectively, were exposed to the solvent (pH 7.2 phosphate buffer). Although the fluorescence emission maximum of Trp residues of type B NT was most blue shifted (331 nm compared to 334 for types A and E NT, and 346 nm for free tryptophan) the fluorescence quantum yields of types A and B were similar and higher than type E. In general the NTs have similar secondary (low α -helix and high β -sheets) and tertiary (exposed tyrosine residues and tryptophan fluorescence quantum yield) structures. Within this generalized picture there are significant differences which might be related to the differences in their biological activities.

Introduction

Botulinum neurotoxins (NT), a group of serologically distinct proteins (~150 kDa) produced by different strains of *Clostridium botulinum*, are responsible for the neuromuscular disease botulism. The NT binds to the neuromuscular junctions, enters the nerve cells, blocks the release of a neurotransmitter, acetylcholine, thus causes flaccid paralysis. The seven serotypes are known as NT types A through G [1–3].

The single chain polypeptide (~150 kDa) undergoes a post synthetic cleavage (nicking) by protease endogenous to the bacteria in some cases (e.g. type

A) but not in others (e.g. type E). The nicked (i.e. dichain) NT has two chains (light and heavy of ~50 and ~100 kDa, respectively) linked through at least one disulfide bond. The NT is therefore recovered from the bacterial cultures as single chain (type E), dichain (type A) or a mixture of single and dichain (type B) molecules. The single chain NTs can be nicked by trypsin into dichain forms [4]. The relatively low toxicity (LD_{50} /mg protein) of newly synthesized NT is enhanced (activated) in the bacterial culture by endogenous protease(s) identity of which is not clear [5]. When the bacterial culture lacks the activation protease(s) e.g. type E, the NT remains unactivated which can be activated 100-fold or more

by trypsin *in vitro*. The activated type E NT remains ~10 fold less toxic than the endogenously fully activated type A [5, 6]. Thus a ~1000 fold difference in toxicity exists between the single chain (unnicked) unactivation type E and the dichain (nicked) activated type A. The partially nicked (i.e. ~10% of the molecules in the dichain form) type B can be activated with trypsin 2–3 fold [7, 8] which is then nearly equal to type A in toxicity. What structural alteration activates the NT is not clear. Nicking does not seem to be the primary cause of activation [4, 8]. Cleavage of another peptide bond (i.e. other than nicking), not yet identified and differences in the conformations between the unactivated and activated NT could be important [4, 7].

Amino acid compositions of the types A, B and E NTs and their respective light and heavy chains are known [9–12]. Comparison of the amino acid contents indicate more similarity among the light chains than the heavy chains [12]. The primary structure of the three NTs are under study [13–15] and only very small segments have been sequenced [12]. The limited sequence data also suggest more homology among the light chains than the heavy chains. Secondary and tertiary structures of the NTs are least known.

Here we report the secondary structure parameters of types A, B and E NT, determined from circular dichroic (CD) spectra, topography of tyrosine residues (in terms of exposure to solvent) determined from second derivative spectra and the state of tryptophan residues based on their fluorescence spectra, and fluorescence quantum yields. The conformational parameters are compared to understand the general pattern of folding of the NT polypeptides and any possible relationship between conformation, single and dichain proteins and levels of toxicities.

Materials and methods

Neurotoxins

Types A, B and E NT were produced and purified as described previously [9–11]. The concentrations (1 mg/ml) of type A, B and E NT were calculated

based on A_{278} of 1.63, 1.85 and 1.4, respectively [12]. All proteins were examined in 10 mM sodium phosphate buffer, pH 7.2.

Absorption and circular dichroism

Absorption and second derivative spectra between 320 and 240 nm spectra were recorded on a single beam DU7 spectrophotometer (Beckman Instruments) at 25°C. The degree of exposed tyrosine residues in the NTs was measured according to Ragone *et al.* [16] using the equation

$$\alpha = (\gamma_n - \gamma_a)/(\gamma_u - \gamma_a)$$

where γ_n is the ratio of the distance between the second derivative spectrum peaks at 284 and 289 (a) to the peaks at 291 and 295 nm (b) when the protein is in its native form (see Fig. 2 for the denotations a and b) whereas γ_u is the ratio of same parameters when the protein is denatured by 6M guanidine·HCl. γ_a is a correction factor calculated on the basis of Tyr to Trp ratio for a given protein [16]

$$\gamma_a = \frac{Ax + B}{Cx + 1}$$

where A, B and C are the constants –0.18, 0.64 and –0.04, respectively (see Table 1 in ref [16]). x is Tyr/Trp ratio for a given protein; for NT A, B and E these values, 4.176, 4.5 and 4.375, respectively, were derived from their amino acid compositions [12]. γ_a values for types A, B and E NT were –0.134, –0.207 and –0.179, respectively.

CD spectra were recorded on a JASCO J-20 A spectropolarimeter at room temperature (23–25°C) as described previously [17]. Secondary structure parameters (α -helix, β -pleated sheet, β -turns and random coils) were calculated according to Chang *et al.* [18] as described previously [17] using mean residue ellipticities between 240 and 190 nm at 1 nm intervals. The mean residue weights for type A, B and E NTs 115.17, 116.12 and 114.49, respectively were calculated from their amino acid compositions [12].

Fluorescence

Spectra were recorded on a SLM 8000 'smart' spectrofluorometer. The excitation wavelength was 295 nm and the spectral resolutions on both excitation and emission monochromators were fixed at 2 nm. All the spectral recordings were carried out at 23–25 °C. Absorbance at 295 nm (excitation wavelength) were kept <0.1 to minimize inner filter effect. For the determination of tryptophan fluorescence quantum yield, fluorescence spectra were recorded between 310 and 410 nm for type A, B and E NTs and free L-tryptophan. The integrated areas of the fluorescence intensity were calculated for a

fixed A_{295} and the tryptophan fluorescence quantum yields of the NTs were estimated relative to the published fluorescence quantum yield of free L-tryptophan [19].

Results

Circular dichroism of type A, B and E NTs

The far UV CD spectra (Figs. 1a, 1b and 1c) show that each NT had double wells at 208 and 217 nm with the negative minima at 212 nm. However, the relative amplitudes of negative maxima were differ-

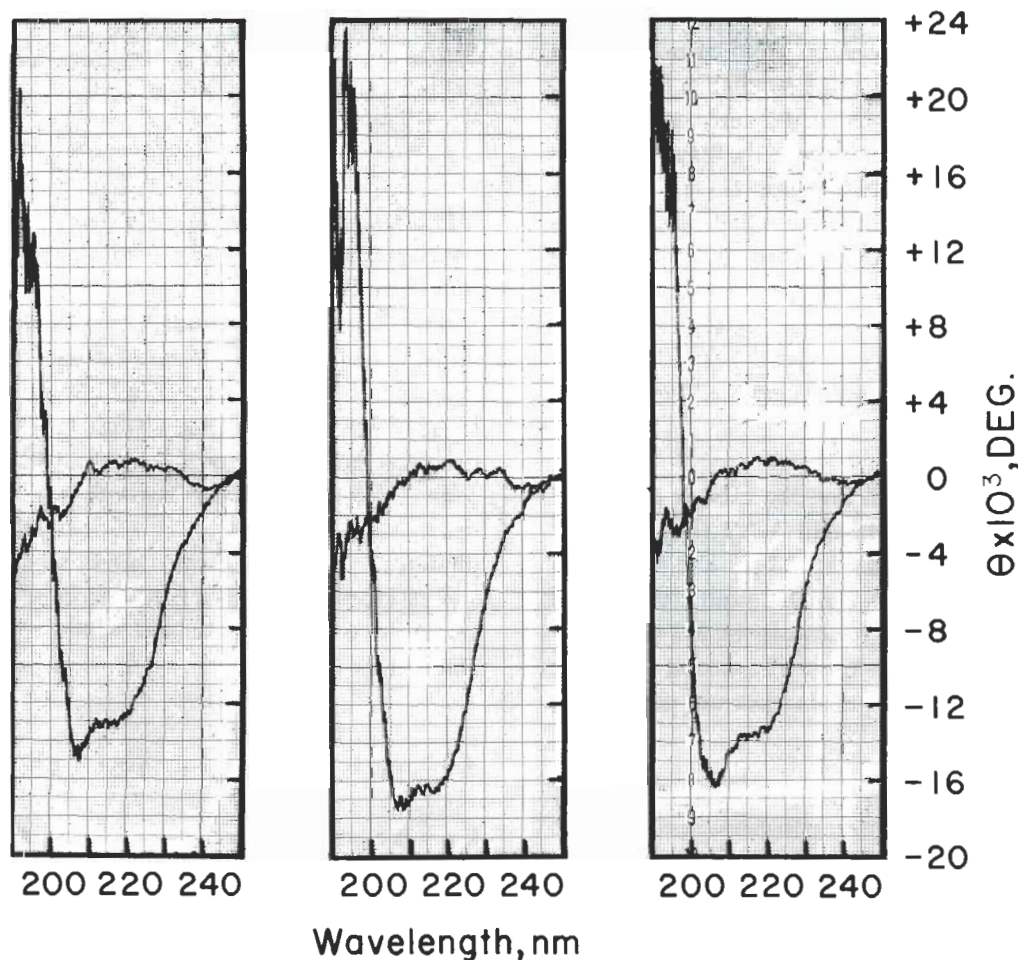


Fig. 1. Typical far UV CD spectra of botulinum NT types A (left panel), B (middle panel) and E (right panel) dissolved in 10 mM sodium phosphate buffer, pH 7.2. The spectra were recorded using a 1 mm pathlength quartz cuvette with protein concentrations of 0.16 mg/ml (type A), 0.15 mg/ml (type B) and 0.17 mg/ml (type E) at room temperature (23–25 °C). Y-axis represents ellipticity θ .

ent for each NT: for example, the negative maxima at 208 nm was stronger in NTs A and E (Fig. 1a and 1c) than in B (Fig. 1b). In A and E NTs, the negative maxima at 217 nm appear like a shoulder. Mean residue ellipticities for A and E NTs were comparable at 208 nm, e.g., $-10,293$ degrees for A and $-10,696$ degrees for E but both were significantly lower than $-12,825$ degrees for B NT.

Secondary structure parameters, calculated based on the far UV CD spectra are shown in Table 1. Two patterns are evident a) while contents of β -pleated sheets were approximately the same in A, B and E NTs, the α -helical contents were not. b) α -helical contents were similar in A and E NT and were $\sim 25\%$ lower than B NT. The significant difference between B and E NT in α -helical contents ($\sim 28\%$ vs. $\sim 21\%$) is accompanied by corresponding difference in random coil contents (sum of α -helix plus random coil 58.7% for B NT vs. 56.8% for E NT). Differences in the contents of β -turns may not be considered important because of the inherent imprecision in the approach of Chang *et al.* [18]. Although β -turn estimation is not reliable their inclusion increases the accuracy of β -pleated sheet determination [18].

Determination of the surface exposed tyrosine residues

The absorption spectra and the overlay of second derivative profile for dichain A NT (Fig. 2) shows the absorption maximum at 278 nm and the second derivative peaks (between 280 and 300 nm) at 285 nm (negative), 289 nm (positive), 292 nm (negative) and 295.5 nm (positive). The second derivative spectra for B (Fig. 3) and E (spectrum not shown)

Table 1. Secondary structure parameters of A, B and E neurotoxins estimated based on the circular dichroic spectra between 240 and 190 nm

	α -helix	β -sheets	β -turns	Random coils
A NT	21.5 ± 1.5	44.0 ± 6.9	4.5 ± 3.9	30.0 ± 1.8
B NT	28.2 ± 1.5	40.5 ± 3.1	1.7 ± 1.8	30.5 ± 3.9
E NT	20.8 ± 0.8	43.2 ± 1.2	0.0	36.0 ± 0.5

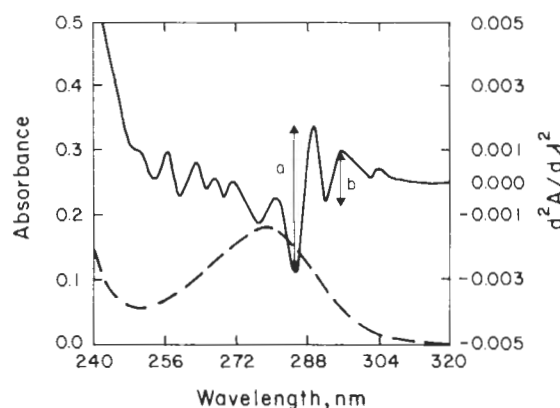


Fig. 2. Absorption (broken line) and second derivative (solid line) spectra of A NT dissolved in 10 mM sodium phosphate buffer, pH 7.2. The absorption spectrum was recorded at 25 °C. The notation 'a' represents the arithmetic sum of the negative $\delta^2A/\delta\lambda^2$ of the peak at 284 nm and the positive $\delta^2A/\delta\lambda^2$ of the peak at 289 nm of the derivative spectrum. The notation 'b' represents the arithmetic sum of the negative $\delta^2A/\delta\lambda^2$ of the peak at 291 nm and positive $\delta^2A/\delta\lambda^2$ of the peak at 295 nm of the derivative spectrum.

NTs are similar. The relative strengths of 295 nm positive peaks were clearly in the order $E < B < A$ NT. The ratios of positive peaks (289/295) for A, B and E NT in their native states were 1.686, 0.811 and 0.724, respectively. Denaturation with 6M guanidine·HCl changed only a little the peak ratio of A NT whereas for B (Fig. 3b) and E NTs, the positive peak ratios changed drastically (Table 2). The peak at 289 is due to both tyrosine and tryptophan residues whereas at 295 it is mostly due to tryptophan residues [16]. The calculated fraction of tyrosine residues of A, B and E NTs exposed to the solvent were 83.5%, 57.6% and 61.0%, respectively (Table 3).

Tryptophan fluorescence quantum yield

From the intrinsic fluorescence spectra of A, B and E NT (Fig. 4) the fluorescence maximum for A and E NT were found at 334 nm compared to 331 nm for B NT (Table 4). The emission maximum of free L-tryptophan was at 346 nm (Fig. 4).

The absolute fluorescence quantum yields estimated for A, B and E NTs based on the published

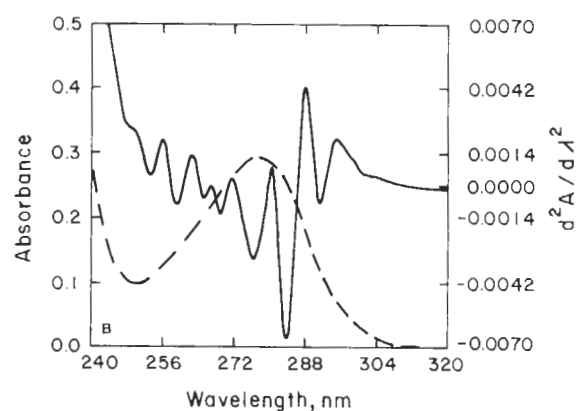
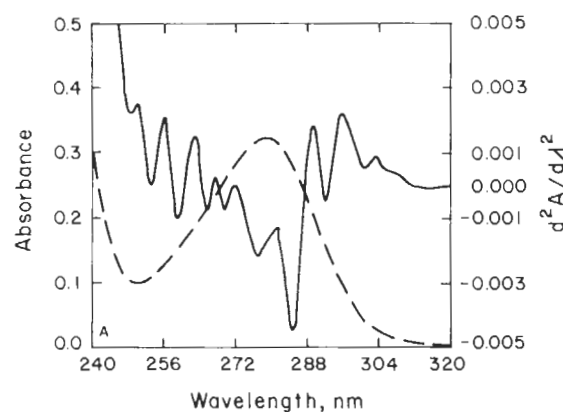


Fig. 3. Absorption (broken line) and derivative spectra (solid line) of B NT (3A) in 10 mM sodium phosphate buffer, pH 7.2 and (3B) in 6M guanidine-HCl. The spectra were recorded at 25°C.

Table 2. Second derivative peak ratios of A, B and E neurotoxins in native and denatured (6M guanidine-HCl) forms

	289/295 (positive peaks)	
	Native	Denatured
A NT	1.686 ± 0.061	1.737 ± 0.334
B NT	0.811 ± 0.091	2.066 ± 0.171
E NT	0.724 ± 0.079	2.273 ± 0.201

Table 3. Degree of tyrosine exposure in A, B and E neurotoxins as determined by the second derivative spectroscopy^a

Neurotoxin	γ_a	γ_u	α	γ_a	α
A	2.895	3.455	4.176	-0.134	$83.5^b \pm 1.3\%$
B	2.499	4.404	4.5	-0.207	$57.6 \pm 1.5\%$
E	2.580	4.335	4.376	-0.179	$61.0 \pm 0.2\%$

^a Calculations according to Ragone *et al.* [16].

^b Average of two different sets of determinations for neurotoxins isolated from two different batches of bacterial cultures.

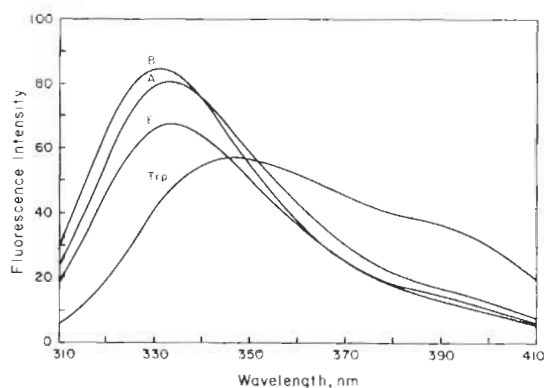


Fig. 4. Fluorescence spectra of free L-tryptophan and tryptophan residues in A, B and E NT dissolved in 10 mM sodium phosphate buffer, pH 7.2 at 23–25°C. Excitation wavelength was 295 nm and the spectral resolutions on both excitation and emission monochromators were 2 nm. The A_{295} values were: 0.060 (type A), 0.055 (type B), 0.060 (type E), and 0.058 (free L-tryptophan).

fluorescence quantum yield for free tryptophan, are listed in Table 4. The quantum yields for A and B NTs were very similar (within experimental error) whereas E NT had lower fluorescence quantum yield (16–21% lower than A or B NT).

Table 4. Intrinsic fluorescence maxima and fluorescence quantum yields of botulinum neurotoxins A, B and E

Sample	Emission maxima	Quantum yield	Relative ratio ^a
A NT	334 ± 1 nm	0.22 ± 0.009	1.16
B NT	331 ± 1 nm	0.23 ± 0.002	1.21
E NT	334 ± 0 nm	0.19 ± 0.012	1.00
Trp	346 ± 2 nm	0.2 ^b	1.05

^a Relative ratios are based on assigning arbitrarily the protein with the lowest quantum yield value of 1.00

^b Taken from Teale and Weber [19].

Related proteins share more of conserved three-dimensional structure than amino acid sequence. Examples include similarities between the nucleotide-binding domain of the dehydrogenases (lactate-, malate-, glyceraldehyde-3-phosphate- and liver alcohol dehydrogenase-) and the lysozyme of hen egg white and T4 bacteriophage [27, 28].

Comparison of intrinsic fluorescence revealed that emission maxima of NTs (331–334 nm) was blue shifted relative to that of free L-tryptophan in aqueous solution (Table 4). Tryptophan emission maximum undergoes blue shift with change in the polarity of the solvent [29]. Blue shifted emission maximum of B NT compared to that of A and E NTs (331 vs. 334 nm) indicates that the fluorescent Trp residues in B NT are in more hydrophobic environment than in A and E NTs. Such differences in the environments of the indole rings may arise from the presence of different side chain groups in the vicinity of tryptophan residues either in the primary structure or from their different topographical positions. The latter situation would arise from a difference in the protein folding. These probable issues can be resolved further when location of all Trp residues in the sequence become known.

The three NTs are similar in their tryptophan content, 17 residues in A, 18 in B and 16 in E NT [12] but their tryptophan fluorescence quantum yields differ significantly (Table 4). The lowest quantum yield of E NT suggests more fluorescence quenching groups in the immediate vicinity of its Trp residues than in A or B NT. The vicinal groups such as the side chains of amino acids can quench the tryptophan fluorescence [29, 30]. While A NT is similar to B in fluorescence quantum yield, A and E are identical in their emission maxima (Table 4). Apparently the protein foldings differ in A, B and E NTs. The differences between the NTs in their emission maxima and the fluorescence quantum yields could be contributed by the heavy, light or both chains. The light chain of A NT has significantly blue shifted emission maximum and considerably lower quantum yield [17] than heavy chain.

To further understand the folding patterns in the A, B and E NTs, topography of the tyrosine residues in these proteins was investigated. The second derivative spectra of NTs were not similar even

though their Tyr/Trp ratios ranged between 4.2–4.5 (i.e., the x values in Table 3). This is probably due to different level of exposure of the chromophores to the solvent or/and due to different micro-environments around the Tyr and Trp residues. Polarity of the solvent is known to alter both λ_{\max} and extinction coefficients of aromatic amino acids [31].

The degree of exposed tyrosine to the same solvent is significantly different in the three NTs: 84% of the 71 Tyr residues in A appeared to be on the surface while ~60% of 81 residues of B and 70 residues of E are on the surface of the protein. Denaturation with 6M guanidine·HCl did not significantly change the peak ratios of A NT; an indication that most of the Tyr residues were already exposed. Such were not the cases in B and E NTs (Table 2). The absolute number of Tyr residues exposed are in the order $A < B < E$ i.e. 59, 47, and 43. This matches the pattern of ~100%, ~10% and ~0% population of the nicked A, B and E NT molecules and also that of the toxicity levels. Whether this correspondence is fortuitous or a reflection of the structure-function relationship requires further study.

The present studies indicate that the secondary and tertiary structural parameters are, in general, similar in A, B and E NTs, although significant differences in α -helical contents, tryptophan fluorescence quantum yields and the degrees of tyrosine exposure (*vide supra*) are noticeable. These observations are consistent with the common pharmacological activity of these NTs having a wide range of potency (see introduction) and distinct antigenicities. None of the structural parameters studied correlate with the toxic potencies among the single chain (E NT) mixture of single and dichain (B NT) and dichain (A NT) which follows the order $A \geq B > E$ NT. This indicates that the structural features of each NT is inherently coded and the degree of toxicity is not dependent on the single or dichain forms. Some of the local conformational features of each NT may be distinct, while others may be common among the NTs. CD, absorption and fluorescence spectra of the whole NT studied are composites of these distinct and common features. Examination of the NTs in several segments (e.g. CD of suitable polypeptide fragments comprising the

entire length of the NT) and prediction from amino acid sequences are likely to reveal local secondary structures. A relationship between local conformational features, toxicity and effect of nicking (single to dichain) may then emerge.

The structural basis of the different toxicity levels could be the conformation near or at the active sites of the NTs. This probability arises from the observed significant differences in the α -helical contents, tryptophan fluorescence quantum yields and the degree of tyrosine exposures in A, B and E NTs. Although the site of action and physiological effects of the NT serotypes are the same their binding sites (localized on heavy chains) do not have identical affinities to the specific receptors [32 and see refs. 17, 18 in 32]. These differences could be due to localized differences in the protein folding among the heavy chains. Because the light chains also have important role in toxicity [32] we are currently comparing the structures of the light chains from different NT serotypes along with their heavy chains.

Acknowledgement

Our sincere thanks to John G. Foley for enthusiastic assistance and for preparing the NT samples. This study was supported in part by NIH grant NS17742, NS24545, Department of Defense-University Research Instrumentation Program award DAAG-29-83-G0063, the Food Research Institute and the College of Agricultural and Life Sciences of the University of Wisconsin-Madison.

References

1. Sakaguchi G: Clostridium botulinum toxins. *Pharmac Ther* 19:165–194, 1983
2. Sugiyama H: Clostridium botulinum neurotoxin. *Microbiol Rev* 44:419–448, 1980
3. Simpson LL: The origin, structure, and pharmacological activity of botulinum toxin. *Pharmac Rev* 33:155–188, 1981
4. DasGupta BR: Structure and structure function relation of botulinum neurotoxins. In: Lewis GE (ed) *Biomedical Aspects of botulism*. Academic Press, New York, 1981, pp 1–19
5. DasGupta BR: Microbial food intoxicants: Clostridium botulinum toxins. In: Rechcigl Jr M (ed) *CRC Handbook of Food-borne Diseases of Biological Origin*, CRC Press, Inc Boca Raton, Florida, 1983, pp 25–55
6. DasGupta BR, Sugiyama H: Biochemistry and pharmacology of botulinum and tetanus neurotoxins. In: Bernheimer AW (ed) *Perspectives in Toxinology*, John Wiley & Sons, New York, 1977, pp 87–119
7. DasGupta BR, Sugiyama H: Molecular forms of neurotoxins in proteolytic *Clostridium botulinum* type B cultures. *Infect and Immun* 14:680–686, 1976
8. Ohishi I, Sakaguchi G: Activation of botulinum toxins in the absence of nicking. *Infect and Immun* 17:402–407, 1977
9. DasGupta BR, Rasmussen S: Purification and amino acid composition of type E botulinum neurotoxin. *Toxicon* 21:535–545, 1983
10. DasGupta BR, Woody M: Amino acid composition of *Clostridium botulinum* type B neurotoxin. *Toxicon* 22:312–315, 1984
11. DasGupta BR, Sathymoorthy V: Purification and amino acid composition of type A botulinum neurotoxin. *Toxicon* 22:415–424, 1984
12. Sathymoorthy V, DasGupta BR: Separation, purification, partial characterization and comparison of the heavy and light chains of botulinum neurotoxin types A, B and E. *J Biol Chem* 260:10461–10466, 1985
13. DasGupta BR, Foley J, Wadsworth C: Botulinum neurotoxin type A: partial sequence of L-chain and its two fragments. *FASEB J* 2:A1750, 1988
14. Gimenez J, Foley J, DasGupta BR: Neurotoxin type E from *Clostridium botulinum* and *C. butyricum*; partial sequences and comparison. *FASEB J* 2:A1750, 1988
15. DasGupta BR, Datta A: Botulinum neurotoxin type B (strain 657): partial sequence and similarity with tetanus toxin. *Biochimie* 70:811–817, 1988
16. Ragone R, Colonna G, Balestrieri C, Servillo L, Irace G: Determination of tyrosine exposure in proteins by second derivative spectroscopy. *Biochemistry* 23:1871–1875, 1984
17. Singh BR, DasGupta BR: Structure of heavy and light chain subunits of type A botulinum neurotoxins analyzed by circular dichroism and fluorescence measurements. *Mol Cell Biochem* (in press) 1988
18. Chang TC, Wu C-SC, Yang JT: Circular dichroic analysis of protein conformation: inclusion of β -turns. *Anal Biochem* 91:13–31, 1978
19. Teale FWJ, Weber G: Ultraviolet fluorescence of the aromatic amino acids. *Biochem J* 65:476–482, 1957
20. Kleffel B, Garavito RM, Baumeister W, Rosenbusch JP: Secondary structure of a channel-forming protein: porin from *E. coli* outer membranes. *EMBO J* 4:1589–1592, 1985
21. Rosenbusch JP: Characterization of the major envelope protein from *Escherichia coli*. Regular arrangement on the peptidoglycan and unusual dodecyl sulfate binding. *J Biol Chem* 249:8019–8029, 1974
22. Shone CC, Hambleton P, Melling J: A 50 kDa fragment from the NH₂-terminus of the heavy subunit of *Clostridium botulinum* type A neurotoxin forms channels in lipid vesicles. *Eur J Biochem* 167:175–180, 1987

23. Blaustein RO, Germann WJ, Finkelstein A, DasGupta BR: The N-terminal half of the heavy chain of botulinum type A neurotoxin forms channels in planar phospholipid bilayers. *FEBS Letters* 226:115–120, 1987
24. Hoch DH, Romero-Mira M, Ehrlich BE, Finkelstein A, DasGupta BR, Simpson LL: Channels formed by botulinum, tetanus, and diphtheria toxins in planar lipid bilayers: relevance to translocation of proteins across membranes. *Proc Natl Acad Sci (USA)* 82:1692–1696, 1985
25. Donovan JJ, Middlebrook JL: Ion-conducting channels produced by botulinum toxin in planar lipid membranes. *Biochemistry* 25:2872–2876, 1986
26. Chou PY, Fasman GD: Empirical predictions of protein conformation. *Ann Rev Biochem* 47:251–276, 1978
27. Rossmann MG, Argos P: Exploring structural homology of proteins. *J Mol Biol* 105:75–96, 1976
28. Matthews BW, Remington SJ, Grutter MG, Anderson WF: Relationship between hen egg white lysozyme and bacteriophage T4 lysozyme: evolutionary implications. *J Mol Biol* 147:545–558, 1981
29. Longworth JW: Luminescence of polypeptides and proteins. In: RF Steiner, I Weinryb (eds) *Excited States of Proteins and Nucleic Acids*, Plenum Press, New York, 1971, pp 319–484
30. Lakowicz JR: *Principles of Fluorescence Spectroscopy*, Plenum Press, New York, 1983, pp 342–385
31. Herskovits TT: Difference spectroscopy. *Methods in Enzymology* 11:748–775, 1969
32. Bandyopadhyay S, Clark AW, DasGupta BR, Sathyamoorthy V: Role of heavy and light chains of botulinum neurotoxin in neuromuscular paralysis. *J Biol Chem* 262:2660–2663, 1987
33. Black SD, Glorioso JC: MSEQ: A microcomputer-based approach to the analysis, display, and prediction of protein structure. *BioTechniques* 4:448–460, 1986

Address for offprints: B.R. DasGupta, Food Research Institute, 1925 Willow Drive, University of Wisconsin, Madison WI 53706, USA